Corrugation-induced transverse voltage in a lateral superlattice

T. Schlösser, K. Ensslin, F. Claro,* and J. P. Kotthaus
Sektion Physik, Ludwig-Maximilians-Universität München, Geschwister Scholl Platz 1, D-80539 München, Germany

M. Holland
Department of Electronics, University of Glasgow, Glasgow G12 8QQ, United Kingdom

R. Ketzmerick
Institut für Theoretische Physik und Sonderforschungsbereich Nichtlineare Dynamik, Universität Frankfurt, D-60054 Frankfurt am Main, Germany

(Received 16 September 1994)

Lateral superlattices are fabricated with a unidirectional potential modulation. The current is passed under an angle α with respect to the lattice direction. In the quantum Hall regime the resistivities, calculated from the respective voltage drops along and perpendicular to the direction of current flow, agree with predictions of tensor calculus. Similar to the Hall effect but in the absence of a magnetic field, a finite voltage drop is detected perpendicular to the current direction. A model based on the ballistic motion of the electrons explains this effect and relates the size of this voltage drop directly to the amplitude of the potential modulation.

I. INTRODUCTION

Lateral superlattices with a potential modulation in one or both lateral dimensions have been realized by various technological means[1] predominantly on $Al_xGa_{1-x}As$-GaAs heterostructures. In these structures the electrons can travel ballistically over several lattice periods, while usually the Fermi wavelength is about an order of magnitude smaller than typical period sizes. For weakly modulated systems the components of the resistivity tensor have been extensively investigated, and various physical phenomena have been observed. In the pioneering work of Weiss *et al.*[2,3] the authors found oscillations in the magnetoresistance for current flow perpendicular to the potential modulation of a unidirectional lateral superlattice. The oscillations are observed in the ballistic transport regime whenever the classical cyclotron diameter becomes commensurate with the superlattice period. These experimental results were explained by the formation of Landau bands and their characteristic magnetic-field-dependent bandwidth.[4,5] In the classical limit, Beenakker showed in an intuitive picture[6] that the $\mathbf{E}\times\mathbf{B}$ drift is modulated as a function of magnetic field in the presence of a lateral superlattice. This way the experimentally observed $1/B$ periodic oscillations can be explained in a quantitative manner by both quantum-mechanical and classical theories.

Similar commensurability effects have also been observed on lateral superlattices with two-dimensional potential modulation,[7,8] as well as on lateral superlattices fabricated on InAs-AlSb quantum wells.[9] The field is now well established, and the theoretical understanding of the experimentally observed effects is based on solid grounds.

In this paper we would like to address the question of how well the tensor picture for the components of the resistivity tensor is obeyed in such experiments. To the best of our knowledge most experiments so far have used measurement geometries where the current flowed either parallel or perpendicular to the main axes of the lateral superlattice. In general, Hall geometries are used where voltage drops perpendicular ($V_\perp$) and parallel ($V_\parallel$) to the direction of current flow can be precisely determined. If the dimension of the Hall bar is much larger than any intrinsic length scale of the system, i.e., the mean free path, lattice period, or Fermi wavelength, one can identify the experimentally determined four-terminal resistance with a particular component of the resistivity tensor ($\rho_\perp$,$\rho_\parallel$), taking into account the underlying geometry of the Hall bar.

Here we fabricate lateral superlattices which are tilted with respect to the direction of current flow as determined by the Hall geometry. In this way the four-terminal resistance measures a mixture of the fundamental resistivities. Since it is difficult to compare measurements on two different samples fabricated independently, we relate various experimental four-terminal resistances obtained on the same Hall geometry for two magnetic-field orientations. Within the experimental accuracy we can explain the resistance traces with the basic tensor relations.

In these symmetry-breaking geometries there occurs a finite voltage drop even at $B=0$ in the direction perpendicular to the current flow. This transverse voltage is directly related to the amplitude of the potential modulation. With a model based on the ballistic motion of the carriers in the potential landscape we can qualitatively explain the observed behavior. In particular this procedure provides a method to estimate the amplitude of the potential modulation which should be a versatile tool especially for future samples with smaller lattice periods.

II. ESTIMATION OF POTENTIAL MODULATION

The fabrication process starts from a GaAs-$Al_xGa_{1-x}As$ heterostructure ($x=0.3$) that is grown by molecular-beam epitaxy and contains a high-mobility two-dimensional electron gas situated 54 nm below the sample surface. At liquid-He temperatures the carrier density is $N_S=3.5\times10^{11}$ cm^{-2} and the mobility is $\mu=450\,000$ cm^2/V s, resulting in an elastic mean free path of the carriers of $\lambda_1=4.4$ μm. A Hall bar is defined by wet etching and provided with Ohmic contacts (AuGe/Ni). Using electron-beam lithography and a suitable development process, the resist is then patterned into an array of wires with period $p=280$ nm whose orientation is well defined with respect to the direction determined by the underlying Hall geometry. The pattern is transferred onto the electron gas either by a carefully tuned wet etching step or by a gate voltage which is applied to a front gate electrode evaporated on top of the patterned resist layer. Both fabrication methods lead to very similar results, and therefore we restrict ourselves to the presentation of experimental data obtained on samples where the lateral superlattice is induced via a patterned gate electrode. The samples are cooled down to liquid-He temperatures $T=4.2$ K, and a magnetic field is oriented perpendicular to the sample surface.

The inset of Fig. 1 (upper right) presents the experimental magnetoresistance (solid line) for a sample where the Hall geometry is oriented such that the current flows perpendicular to the wirelike barriers induced by the gate voltage (see the schematic of the Hall geometry in the upper part of the figure). The well-known commensurability oscillations occur at low magnetic fields $B<0.5$ T, while Shubnikov–de Haas (SdH) oscillations take over at higher magnetic fields. Just after the last maximum at $B\approx0.5$ T that reflects the situation where the classical cyclotron diameter $2R_c$ matches the lattice period, the magnetoresistance rises roughly proportional to B^2. This fact was used by Geim *et al.*[10] to estimate the effective modulation of the superlattice potential. In the present case we fit this parabolic rise of the magnetoresistance as well as the commensurability oscillations (dashed line) to extract a number for the potential modulation of $U_0/E_F=0.09$.

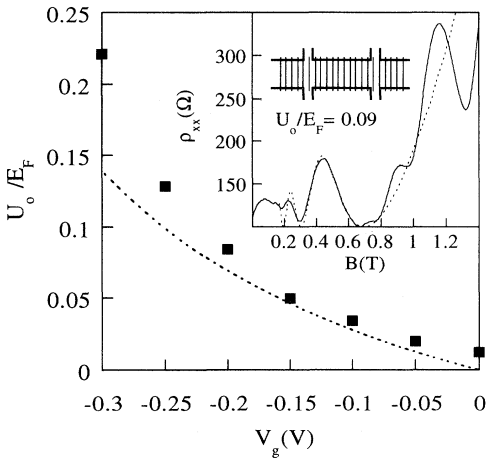

FIG. 1. Inset: The solid line presents an experimental magnetoresistance trace for current flow across the wirelike barriers (see the schematic of the Hall geometry). The dashed line marks a fit to the experimental data according to formulas given in Ref. 10 which lead to the indicated value for the potential modulation. The full squares mark the thus-determined values for the effective potential modulation for different values of the gate voltage. The dashed line indicates the result of the screening calculation [Eq. (1)] as described in the text.

The amplitude of the potential modulation depends on the applied gate voltage as well as on the screening properties, i.e., the average carrier density of the two-dimensional electron gas (2DEG).[11] In order to check our understanding of the potential landscape we have measured the magnetoresistance for a series of gate voltages, and extracted the corresponding potential modulation according to the procedure as described above. The values for U_0/E_F obtained this way are plotted in Fig. 1 as a function of gate voltage. The carrier density is obtained from the numerical relation N_S (10^{11} cm^{-2})$=2.94+4.96V_g$ (V) which is determined from the experiment. The Fermi energy is obtained from the carrier density via the constant density of states of the 2DEG. This assumption is justified as long as the potential modulation is small, $U_0/E_F\ll1$. The calculation by Kotthaus and Heitmann[11] assumes a sinusoidally modulated potential at the sample surface. A more realistic approach by Winkler[12] relies on a sinusoidally modulated electron density on the sample surface leading to a different numerical factor C in the equation

$$\frac{U_0}{E_F}=C\frac{N_g}{N_s}\frac{1}{1+p/s} \tag{1}$$

of Winkler.[12] Here N_g is the charge deposited on the gate, and C is a numerical factor which contains the dielectric constants of the semiconductors and the photoresist and the efficiency of the grating gate. The last factor describes the screening properties of the 2DEG (Ref. 13) with the constant screening length in GaAs of $s=30$ nm. The results of this calculation are indicated by the dashed line in Fig. 1. The overall agreement with the experimentally obtained data for the potential modulation is satisfactory. One has to keep in mind that some sample parameters such as the Schottky barrier height or the aspect ratio of the photoresist grating are not precisely known. This leads, for example, to the experimentally observed finite value for U_0/E_F at $V_g=0$. Furthermore, for very negative values of the gate voltage, the extracted value of U_0/E_F exceeds the estimation of Eq. (1). In this regime, where the potential modulation is already fairly strong, the simple fitting procedure to the experimental ρ_{xx} traces with the formulas as given in the literature for weak potential modulation[4–6] is not strictly valid any more. In particular, the assumption of a constant scattering time independent on the location of the electron in the superlattice potential is no longer applicable. Nevertheless we conclude that our overall understanding of the potential landscape relying on classical ballistic

electron transport leads to results that are in agreement with basic screening calculations.

III. FINITE TRANSVERSE VOLTAGE IN THE TILTED GEOMETRY

In this section we describe experiments where the direction of the lateral superlattice is tilted with respect to the main axes of the Hall geometry. A typical schematic is presented in the inset of Fig. 2 (upper left corner), where the current can be passed along two directions which are perpendicular to each other. Very naively one expects a voltage drop perpendicular to the direction of the current flow, because the electrons are deflected by the presence of the tilted potential. An intuitive analog is the Gedanken experiment, where a pin ball rolls down a tilted washboard. This ball will not follow the direction of its initial velocity but will be deflected compared to a flat surface. This can be seen in Fig. 3 for an electron trajectory in a tilted 1D potential.

We fabricated a sample where the potential with unidirectional modulation is tilted with respect to the direction of the current flow. The angles are 30° and 60°, respectively, for a Hall geometry with two perpendicular arms, as sketched in the inset of Fig. 2. The measured transverse resistivity ρ_{xy} at $B=0$ is presented in Fig. 2 (the inset in the upper right corner) as a function of the gate voltage applied to the corrugated gate electrode (solid line: $\alpha=30°$, dashed line: $\alpha=60°$). For negative gate voltages the transverse resistivity ρ_{xy} increases. This is obviously related to the increased potential modulation and therefore the enhanced deflection of the electrons from their ballistic path along the respective direction of the current flow.

Let us now consider what one would expect for the results of a tensor calculation. The resistivities for the current flow perpendicular and parallel to the wire grating are denoted by $\rho_\perp$ and $\rho_\parallel$, respectively. The tensor in this axes system (x',y') (see Fig. 3) therefore reads

$$\underline{\rho}'=\begin{pmatrix}\rho_\perp & -\rho_H\\ \rho_H & \rho_\parallel\end{pmatrix}. \tag{2}$$

The off-diagonal components ρ_H, i.e., the Hall effect, are antisymmetric because of the Onsager-Casimir relations that hold in this system.[14,15] The validity of these symmetry relations for the Hall effect have been proven experimentally in rectangular antidot lattices.[16,17] If the resistivity tensor is rotated by the angle α with the matrix

$$\underline{D}=\begin{pmatrix}\cos\alpha & \sin\alpha\\ -\sin\alpha & \cos\alpha\end{pmatrix}, \tag{3}$$

the resulting tensor $\underline{\rho}=\underline{D}\underline{\rho}'\underline{D}^T$ in the coordinate system (x,y) is given by

$$\underline{\rho}=\begin{pmatrix}\rho_{xx} & \rho_{xy}\\ \rho_{yx} & \rho_{yy}\end{pmatrix}=\begin{pmatrix}\rho_\perp\cos^2\alpha+\rho_\parallel\sin^2\alpha & -\rho_H+(\rho_\parallel-\rho_\perp)\sin\alpha\cos\alpha\\ \rho_H+(\rho_\parallel-\rho_\perp)\sin\alpha\cos\alpha & \rho_\perp\sin^2\alpha+\rho_\parallel\cos^2\alpha\end{pmatrix}. \tag{4}$$

At $B=0$ ($\rho_H=0$) one finds $\rho_{xy}=\rho_{yx}=(\rho_\parallel-\rho_\perp)\sin\alpha\cos\alpha$. In other words the finite transverse voltage that drops perpendicularly to the direction of current flow is directly proportional to the difference between the resistivities along the two main axes of the lateral superlattice. The term $\sin\alpha\cos\alpha$ is symmetric with respect to $\alpha=45°$. We therefore expect that the transverse voltage for $\alpha=30°$ and 60° should be the same. This is definitely not the case for the data presented in the inset in Fig. 2. Experimentally a different Hall geometry is probed for a different tilt angle. Since the transverse resistivity ρ_{xy} is found to be very sensitive to the details of a particular sample and its potential modulation, it is not surprising that the experimental results do not follow the predicted behavior. However, we find ρ_{xy} to be always larger for $\alpha=60°$ than for $\alpha=30°$. We suspect the reason for this observation to be the nonuniformity of the electron distribution in phase space, as discussed at the end of this section.

The tensor relations as discussed above rely solely on fundamental symmetry relations. A quantitative comparison with the experimental features requires a microscopic transport model that relates the longitudinal and transverse resistances on the same Hall bar. Let us assume a potential induced by a negative gate voltage of the form $U(x')=U_0[1+\sin(2\pi x'/p)]$ in the x' direction, rotated by an angle α from the direction of the Hall bar (Fig. 3).

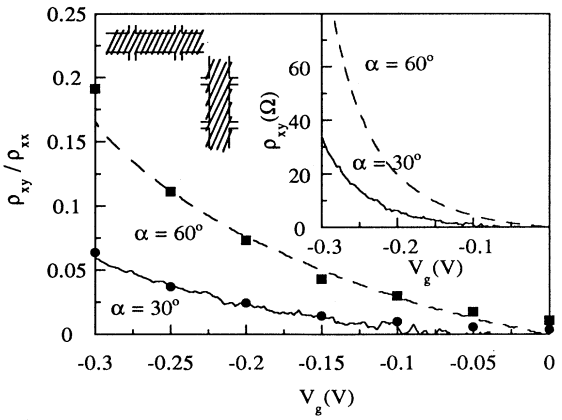

FIG. 2. The inset in the upper right corner shows the transverse resistivity ρ_{xy} as a function of gate voltage measured at $B=0$ for a geometry as shown in the upper left corner. The two lines mark the results for the two current orientations as indicated. The solid and dashed curves in the main figure represent the calculated ratios of the transverse (ρ_{xy}) and longitudinal resistivities (ρ_{xx}, evaluated with the known width to length ratio of the Hall geometry) measured on the two Hall geometries. The dots and squares are calculated using the resistivities of Eq. (10), the known potential modulation from Fig. 1, and the respective tilt angle.

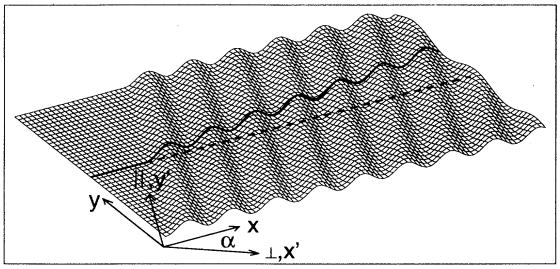

FIG. 3. Electron trajectory in a 1D potential modulation tilted by an angle α in a Hall bar. The potential deflects the trajectory from the direction it would have if there were no potential modulation (dashed line). This explains the experimentally found transverse resistance ρ_{xy} in Fig. 2. The two coordinate systems (x,y) and (x',y') rotated by the angle α are shown.

The electrons may travel at the minimum of the potential ($x_0'=-p/4$) with the velocity $v_0=\sqrt{2E_F/m}$ in the direction of the Hall bar. Their dynamics perpendicular (x') and parallel (y') to the potential modulation is decoupled, and energy conservation in x' direction requires

$$\tfrac{1}{2}mv_\perp^2(x')+U(x')=\tfrac{1}{2}mv_0^2\cos^2\alpha+U(x_0') \ . \tag{5}$$

We assume that the electron travels ballistically over the potential landscape following the ups and downs of the washboard potential. The time it takes for an electron to transverse a lattice constant in the perpendicular direction can be calculated as

$$\begin{aligned}\tau_\perp &= \int_\xi^{\xi+p}\frac{dx'}{v_\perp(x')} \\ &= \int_\xi^{\xi+p}dx'\left[v_0^2\cos^2\alpha-\frac{2U(x')}{m}\right]^{-1/2} \\ &= \Gamma\int_0^p dx'[1-r\sin(2\pi x'/p)]^{-1/2} \ ,\end{aligned} \tag{6}$$

using the abbreviations $\Gamma=(v_0^2\cos^2\alpha-2U_0/m)^{-1/2}$ and $r=U_0/(mv_0^2\cos^2\alpha/2-U_0)$. The parameter r depends on the relative magnitude of the potential modulation U_0 and the kinetic energy across the potential hills. For our present experiment the potential modulation is considered weak, i.e., $U_0\ll E_F$ leading for fixed $\alpha\neq 90°$ to $r\ll 1$. With K being the complete elliptic integral of the first kind, $\tau_\perp$ can be written as

$$\begin{aligned}\tau_\perp &= \frac{2p\Gamma}{\pi\sqrt{1+r}}K\left[\left(\frac{2r}{1+r}\right)^{1/2}\right] \\ &= p\Gamma\left[1+\frac{3r^2}{16}+\cdots\right] \\ &\approx \frac{p}{v_0\cos\alpha}\left[1+\frac{U_0}{mv_0^2\cos^2\alpha}\right] \ .\end{aligned} \tag{7}$$

From this result we can derive a relation between the measured longitudinal and Hall resistances of the tilted geometry. To this end we calculate the average velocities in the x and y directions of the trajectory in Fig. 3 by using the matrix $\underline{D}$ [Eq. (3)] to rotate the average velocities perpendicular $v_\perp=p/\tau_\perp$ and parallel $v_\parallel=v_0\sin\alpha$ to the potential modulation. We find

$$v_x=v_0\left[1-\frac{U_0}{2E_F}\right], \quad v_y=v_0\tan\alpha\frac{U_0}{2E_F} \ , \tag{8}$$

and thus, to lowest order in U_0/E_F,

$$v_y=v_x\tan\alpha\frac{U_0}{2E_F} \ . \tag{9}$$

We include impurity scattering by assuming that under a small electric field applied in the x direction the drift velocities obey the same relation. This gives the conductivity tensor, and by inversion we find, to lowest order in U_0/E_F,

$$\rho_{xy}=\rho_{xx}\tan\alpha\frac{U_0}{2E_F} \ . \tag{10}$$

This formula directly relates the transverse and longitudinal resistivities of a particular Hall geometry via the effective potential modulation. The derivation is only applicable for small potential modulation and, in particular, if the kinetic energy across the wirelike barriers is much larger than the barrier height. In the spirit of Eq. (10) we plot the ratio of transverse and longitudinal resistances for the two Hall geometries in Fig. 2. From Fig. 1 it is possible to estimate the potential modulation for a given gate voltage. This value is taken, divided by two, and multiplied by the tangent of the respective tilt angle [see Eq. (10)]. The solid squares and circles in Fig. 2 mark the result of this calculation, in surprising agreement with experimental data. Not all samples reveal such a good compliance between the two approaches of extracting a potential modulation, but considering the crudeness of our model anything within a factor of 2 would be satisfactory.

The angular dependence predicted by our model [Eq. (10)] does not agree with the results of the tensor calculation [Eq. (4)]; however, it fits the experimental results much better (Fig. 2). This is due to the fact that in the model just a single trajectory is considered, whereas the tensor calculation implicitly assumes a uniform phase-space density and thus an averaging over all initial conditions.

The result for ρ_{xy} in Eq. (10) depends sensitively on the starting condition x_0' for the electron. If the electron were to start in the middle of the potential at $x_0'=0$ in the x direction, the value for ρ_{xy} would be smaller, as for symmetry reasons the linear term in U_0/E_F vanishes and only a quadratic term survives. On the other hand, for a starting condition at a maximum ($x_0'=p/4$) of the potential the transverse resistivity ρ_{xy} would even have a different sign, which we never observed in the experiment. We find that an averaging over all starting positions and directions using the Kubo formula recovers the angular dependence of the tensor calculation.[18]

As experiments were done on Hall bars only a few

times larger than the electron mean free path, we believe that the implicit assumption of a uniform phase-space density for the tensor calculation as well as for the Kubo formula is not fulfilled. This explains the success of our model considering only the intuitively most important trajectory. We plan to investigate this point in more detail in the future, e.g., by using Hall bars of different sizes.[18]

IV. ANISOTROPIES IN THE QUANTUM HALL REGIME

Let us now turn to the discussion of the properties of the broken symmetry geometries in finite magnetic fields. For small potential modulations $U_0/E_F < 0.05$ the SdH oscillations are perfectly periodic in $1/B$, and one can extract an average carrier density. Also the quantum Hall plateaus that are experimentally observed on a sample with a tilted lateral superlattice are almost indistinguishable from those of an unpatterned sample with the same carrier density. However, for a stronger potential modulation the resistivities parallel and perpendicular to the direction of current flow become mixed more strongly and other features arise. Figure 4(a) presents experimental data (solid line) for the Hall resistance measured on a Hall geometry where the lateral superlattice is tilted under an angle of 60° with respect to the direction of current flow. We estimate the relative potential modulation to be about $U_0/E_F \approx 0.22$ for this particular gate voltage. The finite transverse resistance at $B=0$ is not resolved on this scale. The other solid line in Fig. 4(a) is recorded with the direction of the magnetic field reversed. It is obvious that the two experimental traces exhibit oscillatory features which, however, show no indication of a quantum Hall plateau. In particular we observe negative values of ρ_{xy} for one magnetic-field orientation. In order to extract the antisymmetric component of these experimentally obtained resistances, we calculated $\rho_{as}=1/2[\rho_{xy}(B\uparrow)-\rho_{xy}(B\downarrow)]$, which results in the dotted line in Fig. 4(a). This trace exhibits a linear behavior at low fields and a well-pronounced quantum Hall plateau at $B \approx 3$ T. This is expected from the tensor relations as given above. In contrast to Sec. III, here experimental traces obtained on one Hall geometry are compared, and the agreement with the theoretical predictions is therefore quantitative.

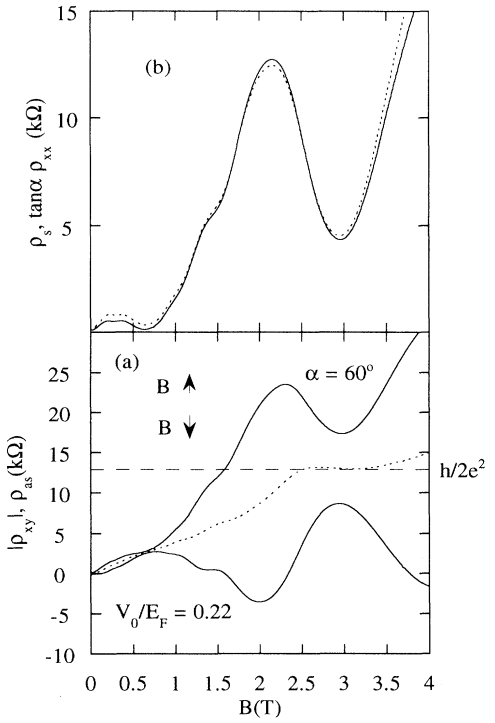

FIG. 4. (a) Hall resistance ρ_{xy} (solid lines) measured on one Hall geometry (as in the inset of Fig. 2, $\alpha=60°$) for two magnetic-field orientations which are reversed with respect to each other. The gate voltage is at $V_g=-300$ mV, resulting in an estimated potential modulation of $V_0/E_F=0.22$ (see Fig. 1). The dashed line is the result of a calculation that extracts the antisymmetric parts ρ_{as} of both measurements. (b) The solid line shows the result of a calculation that extracts the symmetric parts ρ_s of the experimental Hall resistances from (a). The dashed line shows an experimental magnetoresistance ρ_{xx} from the same Hall geometry which is multiplied by $\tan 60°=1.73$ as described in the text.

This way we can also extract the symmetric components of the experimentally determined Hall resistances $\rho_s=1/2[\rho_{xy}(B\uparrow)+\rho_{xy}(B\downarrow)]$, which is displayed in Fig. 4(b) by the solid line. For a strong potential modulation and high magnetic fields $\rho_\perp \gg \rho_\parallel$, the tensor relations can be modified as follows: $\rho_s=\rho_\perp \sin\alpha \cos\alpha$ and $\rho_{xx}=\rho_\perp \cos^2\alpha$. For $\alpha=60°$ one obtains $\rho_s/\rho_{xx}=\tan\alpha=\tan 60°=1.73$. The value of ρ_{xx} is measured and plotted accordingly in Fig. 4(b) (dashed line). The overall agreement with the solid line is excellent, which again hints at the validity of the tensor relations. We can thus quantitatively compare resistance traces that are obtained by very different measurements on the same Hall geometry.

V. CONCLUSIONS

Generally the resistivities of a two-dimensional electron gas are proportional to the experimentally determined four-terminal resistances. This is valid even for 2DEG's with a superimposed lateral superlattice as long as the internal length scales of the system (lattice period, mean free path, phase-coherence length) are short compared to the external dimensions of the Hall geometry.

Here we have described transport experiments on samples where the orientation of the lateral superlattice is tilted with respect to the direction of current flow defined by the Hall geometry. We observe a finite transverse voltage at $B=0$ occurring perpendicular to the direction of current flow. The size of this transverse resistance can be related to the magnitude of the relative potential modulation. The value of the potential modulation can be extracted from a fitting procedure to the classical commensurability oscillations, in agreement with a theoretical analysis. We present a model relying on ballistic electron transport through the potential landscape explaining the sign, magnitude, and angular dependence of the transverse voltage.

At high magnetic fields the behavior of the Hall effect

depends on the direction of the magnetic field. By suitably adding various four-terminal resistances that are experimentally determined on the same Hall geometry, the properties of well-quantized Hall plateaus can be recovered. In particular we can relate the magnetoresistance to the symmetric part of the Hall resistance in simplifying the corresponding tensor relations. If one considers experimental results obtained on one and the same Hall geometry the tensor relations for the resistivity tensor can be confirmed experimentally.

If experimental results from different samples are compared the situation is more complex, as the potential modulation depends very sensitively on the details of the fabrication process. However, with our model we can estimate the order of magnitude of the potential modulation. This has important consequences for future samples with smaller periodicities. In that case it will be more difficult to fit the commensurability oscillations with the classical formula. We expect that the broken-symmetry geometries presented in this paper will help to clarify the situation since the basic symmetry properties should persist from the classical into the quantum regime.

ACKNOWLEDGMENTS

It is a pleasure to thank W. Hansen, A. Lorke, F. P. Salzberger, R. Schuster, S. Ulloa, and R. Winkler for most valuable discussions. We are grateful to the Deutsche Forschungsgemeinschaft and the ESPRIT Basic Research Action for financial support.

*Permanent address: Universidad Catolica de Chile, Santiago, Chile.

[1]For a review, see W. Hansen, U. Merkt, and J. P. Kotthaus, in *Nanostructured Systems,* edited by M. Reed, Semiconductors and Semimetals Vol. 35 (Academic, San Diego, 1992), p. 279.

[2]D. Weiss, K. v. Klitzing, K. Ploog, and G. Weimann, in *High Magnetic Fields in Semiconductor Physics II,* edited by G. Landwehr (Springer, Berlin, 1988), p. 357.

[3]D. Weiss, K. von Klitzing, K. Ploog, and G. Weimann, Europhys. Lett. **8**, 179 (1989).

[4]R. R. Gerhardts, D. Weiss, and K. v. Klitzing, Phys. Rev. Lett. **62**, 1173 (1989).

[5]R. W. Winkler, J. P. Kotthaus, and K. Ploog, Phys. Rev. Lett. **62**, 1177 (1989).

[6]C. W. J. Beenakker, Phys. Rev. Lett. **62**, 2020 (1990).

[7]D. Weiss, K. von Klitzing, K. Ploog, and G. Weimann, Surf. Sci. **229**, 88 (1990).

[8]A. Lorke, J. P. Kotthaus, and K. Ploog, Superlatt. Microstruc. **9**, 103 (1991).

[9]T. Utzmeier, T. Schlösser, K. Ensslin, J. P. Kotthaus, C. R. Bolognesi, C. Ngyuen, and H. Kroemer, Solid-State Electron. **37**, 575 (1994).

[10]A. K. Geim, R. Taboryski, A. Kristensen, S. V. Dubonos, and P. E. Lindelof, Phys. Rev. B **46**, 4324 (1992).

[11]J. P. Kotthaus and D. Heitmann, Surf. Sci. **113**, 481 (1982).

[12]R. W. Winkler, Diploma thesis, University of Hamburg, 1989.

[13]F. Stern and W. E. Howard, Phys. Rev. **163**, 816 (1967).

[14]L. Onsager, Phys. Rev. **37**, 405 (1931); **38**, 2265 (1931).

[15]H. B. G. Casimir, Rev. Mod. Phys. **17**, 343 (1945).

[16]R. Schuster, K. Ensslin, J. P. Kotthaus, M. Holland, and C. Stanley, Phys. Rev. B **47**, 6843 (1993).

[17]K. Ensslin and R. Schuster, in *III-V Semiconductor Quantum Systems, 1995,* edited by K. Ploog (The Institution of Electrical Engineers, London, 1995).

[18]T. Schlösser, K. Ensslin, J. P. Kotthaus, R. Ketzmerick, and T. Geisel (unpublished).